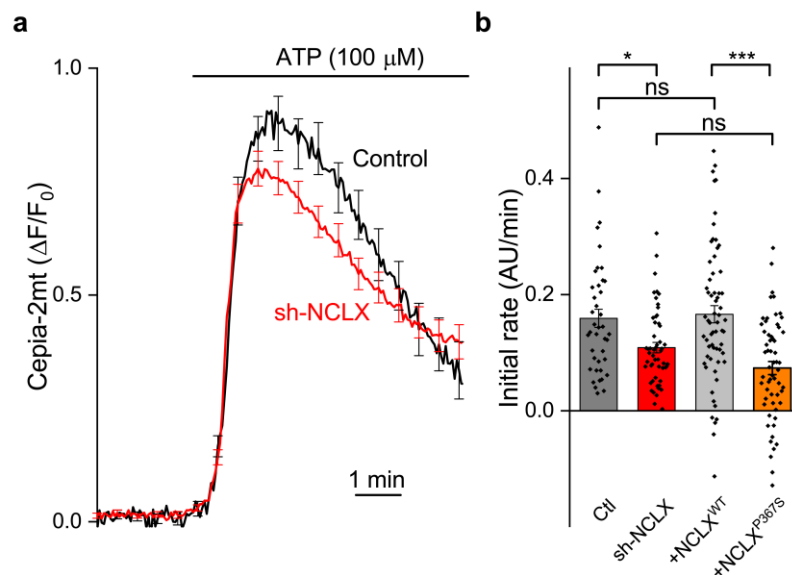


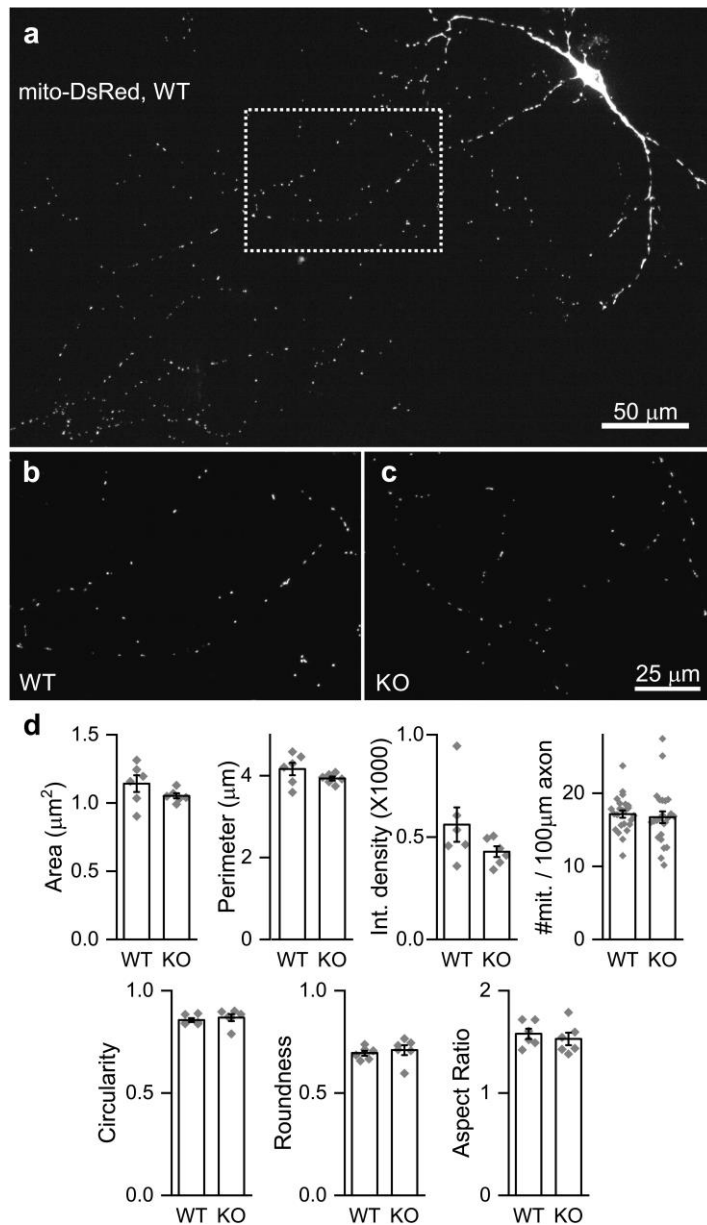
## Supplementary Figures and Legends



**Supplementary Fig. 1: Knock-down of NCLX in SH-SY5Y cells slows mitochondrial calcium efflux.**

**a** *Cepia2-mt* was expressed in SH-SY5Y cells (black) or in cells in which the endogenous NCLX was knocked down by shRNA (red), and mitochondrial transients (*Cepia2-mt* fluorescence) were induced by bath application of ATP (horizontal line). Shown are mean $\pm$ SEM traces ( $n=41$  and  $53$ , respectively).

**b** Linear fit of a 150 seconds period after calcium levels started to decline served to determine the initial calcium efflux rate. Shown are extrusion rates extracted from data in graph in **a** and Fig. 1f ( $0.159\pm 0.016$ ,  $0.109\pm 0.009$ ,  $0.166\pm 0.016$ ,  $0.073\pm 0.011$  arbitrary units/minute). Efflux rates differed between the experimental groups (Kruskal Wallis ANOVA, \*\*\*  $p=3e-6$ , chi-square=28.72, DF=3; post-hoc pairwise comparisons using the Mann-Whitney *u*-test with Bonferroni's correction). KD of NCLX reduced the efflux rate compared to control (\*  $p=0.048$ ), which was rescued by reintroduction of WT NCLX ( $p>0.05$  vs. control), but not by the P367S variant ( $p>0.05$  vs. KD), for which the efflux rate was significantly lower than compared to WT NCLX (\*\*\*)  $p<0.001$ .



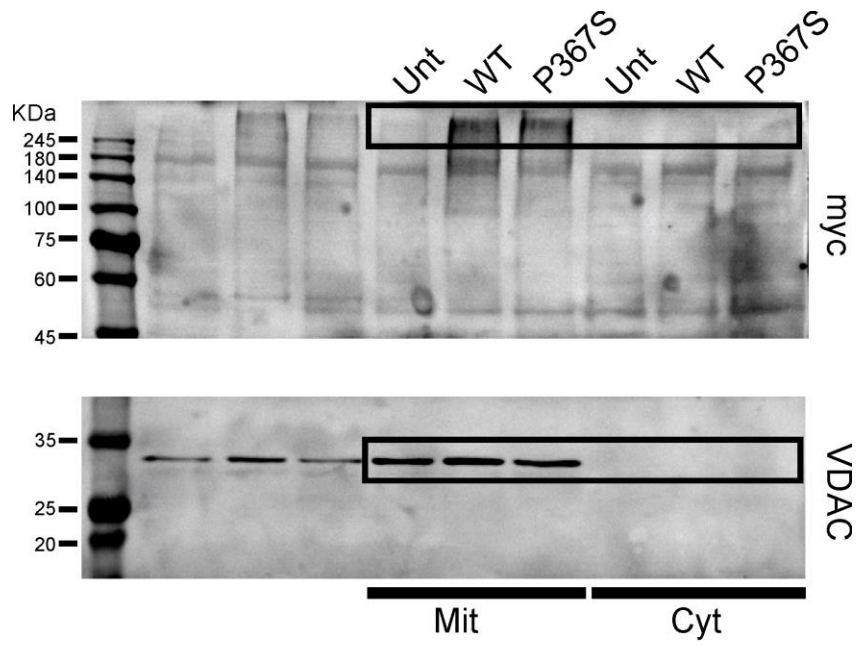
**Supplementary Fig. 2: Deletion of NCLX does not alter mitochondrial morphology in axons of cultured hippocampal neurons.**

**a** Cultured hippocampal neurons were sparsely transfected with plasmids for the expression mito-DsRed, and were imaged at DIV 14 to visualize mitochondria. Representative image of a WT neuron, showing the cell body, primary dendrites and an axonal arbor.

**b** Magnification of rectangle in **a**. Shown are axonal mitochondria, identified by their compact size and by their localization in a neurite far from the cell body.

**c** Representative image of axonal mitochondria in an NCLX KO neuron, to the same scale as in **b**.

**d** Quantification of parameters related to mitochondrial size (area, perimeter length, integrated density), number of mitochondria per 100 $\mu\text{m}$  of axon, and shape (circularity, roundness, long to short axis aspect ratio). Symbols represent the average of each parameter in independent pictures ( $n=6,6$  pictures of WT and KO axons, 80-500 mitochondria per picture), except for mitochondrial counts, for which  $n=24,24$ . Bars and error bars represent mean $\pm$ SEM values. No significant differences were observed between the genotypes for all properties ( $p>0.16-0.65$ , two-tailed Students' *t*-tests).



**Supplementary Fig. 3: Full blots of data shown in Fig. 1d.** Unt: untransfected, WT: myc-NCLX<sup>WT</sup>, P367S: myc-NCLX<sup>P367S</sup>, Mit: mitochondrial fraction, Cyt: cytoplasmic fraction, KDa: Kilo Dalton. Primary antibody indicated on right. Boxes denote the blots shown in Fig. 1d. Panels originate from the same blot, which was cut just below the 45 KDa marker.